

# Flexy: Shape-Customizable, Single-Layer, Inkjet Printable Patterns for 1D and 2D Flex Sensing

Nirzaree Vadgama

Saarland University  
Saarland Informatics Campus  
Saarbrücken, Germany  
nirzaree.svnit@gmail.com

Jürgen Steimle

Saarland University  
Saarland Informatics Campus  
Saarbrücken, Germany  
steimle@cs.uni-saarland.de

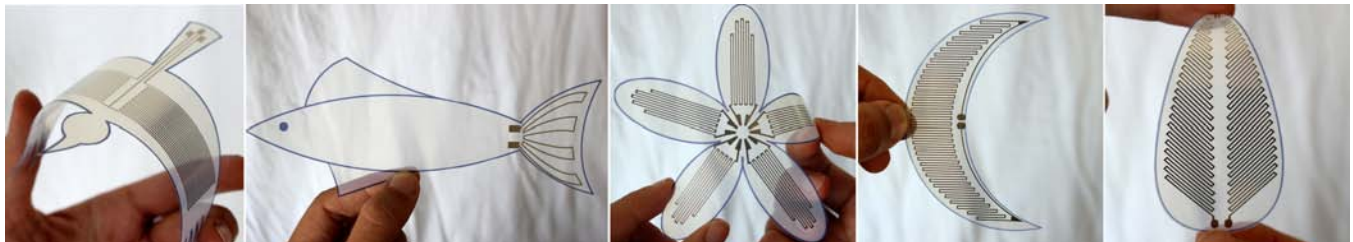


**Figure 1.** Flexy enables designers and makers to easily, quickly and cheaply realize thin physical objects in custom shapes that feature an embedded deformation sensor. This enables a wide range of interactive applications with deformable surfaces.

## ABSTRACT

We contribute a new technique for fabricating highly customized 1D and 2D flex sensing surfaces on thin and flexible substrates. It enables designers and makers to easily, quickly and inexpensively realize thin physical objects in custom shapes with an embedded deformation sensor. The deformation sensor is digitally designed and then fabricated with a single layer of conductive material in a single pass, using an off-the-shelf inkjet printer. We establish a design space and investigate how to realize flex sensing surfaces of highly varied geometries. In a technical evaluation, we demonstrate the technical feasibility of such sensors and investigate their response. Lastly, we demonstrate the practical applicability for tangible interfaces by presenting five example applications.

## Author Keywords

Flexible sensor; conductive inkjet printing; deformable input devices; digital fabrication; rapid prototyping.

## ACM Classification Keywords

H.5.m. Information interfaces and presentation.

## INTRODUCTION

Flexible and deformable user interfaces are of increasing interest to the HCI research and interaction design

communities. Advances in sensing and output technologies and miniaturization of electronics enable very thin, lightweight, and deformable form factors [19, 15, 20, 29, 12]. These open up a new space of intuitive physical interactions [9, 21, 33, 35, 26, 16, 30]. Moreover, varied and highly custom form factors allow for physical interactions that are tailored to the specific shape of the user interface [27, 32].

An important question for realizing interactive prototypes is how to sense deformations. Using external optical sensing limits mobility [14, 35]. Creating prototypes with commercially available flex sensors results in rather thick and not very deformable prototypes [21, 23, 37]. Printed deformation sensors offer the benefit of a very slim form factor and high deformability. However, existing approaches are either very complicated to fabricate and interface for HCI researchers and designers [29] or they are restricted to sensing of only coarse and discrete deformations [15].

We contribute a new technique for fabricating highly customized 1D and 2D flex sensing surfaces. It enables designers and makers to easily, quickly and inexpensively realize thin physical objects in custom shapes featuring an embedded deformation sensor. The technique is based on conductive inkjet printing [19] and on the basic sensing principle of resistive strain gauges.

While conductive inkjet printers are now getting widely used in HCI labs, it is unclear thus far if and how well this inexpensive and fast printing technology would allow for resistive sensing of deformations. In addition, printing and patterning approaches offer a lot of freedom in how conductive traces can be laid out. This enables an unprecedented geometric variety of sensor layouts, including highly varied sizes, arrangements, and shapes of sensors.

Permission to make digital or hard copies of all or part of this work for personal or classroom use is granted without fee provided that copies are not made or distributed for profit or commercial advantage and that copies bear this notice and the full citation on the first page. Copyrights for components of this work owned by others than the author(s) must be honored. Abstracting with credit is permitted. To copy otherwise, or republish, to post on servers or to redistribute to lists, requires prior specific permission and/or a fee. Request permissions from [Permissions@acm.org](mailto:Permissions@acm.org).  
TEI '17, March 20 - 23, 2017, Yokohama, Japan  
Copyright is held by the owner/author(s). Publication rights licensed to ACM.

ACM 978-1-4503-4676-4/17/03\$15.00

DOI: <http://dx.doi.org/10.1145/3024969.3024989>

This has the potential to open up a new design space for deformable user interfaces of very custom shapes.

In this paper we investigate the design space of easy-to-fabricate resistive flex sensors to support 1D and 2D flex sensing on deformable surfaces. Based on this design space, we will demonstrate how to realize flex sensing surfaces of highly varied geometry. Moreover, the design space allows to provide recommendations for interface designers on how to design such flex sensors for their interface prototypes.

In a technical evaluation, we demonstrate the technical feasibility of such sensors, investigating the response of these sensors for various dimensions and various types of deformations. Lastly, we demonstrate the practical applicability for tangible interfaces by presenting five example applications.

The main contributions of this paper are as follows:

- 1) We present a shape-customizable single layer pattern for flex sensing and introduce a design space. The pattern can sense single as well as multi-axial bending deformations. The design can be customized by adapting parameters of several primitives; this results in a wide range of geometries that can be augmented with the pattern. The flex sensor is fabricated through fast and inexpensive conductive inkjet printing.
- 2) We present spatial arrangements of the sensor design in 1D & 2D for sensing surface deformations, in varied sensor geometries. For sensing more complex deformations of a 1D surface, a linear array of sensing units is presented. A radial array enables sensing of 2D deformations on a surface.
- 3) We contribute results from a technical evaluation and present a set of practical application examples to demonstrate the feasibility of the approach.

## RELATED WORK

Embedded flex sensors are commonly constructed using fabric, fiber optic or functional ink materials [6]. Fabric-based flex sensors are constructed by sandwiching a piezoresistive material between layers of conductive fabric [2]. Such a sensor design is primarily designed for pressure sensing; however it can also measure pressure as a function of flexion, thereby acting as a flex sensor. An optical bend sensor [9, 17] consists of pairs of light emitters and receivers, which are connected by an optical fiber. The intensity of the received signal varies in proportion to fiber bending. Shapetape [9], a bendable and twistable input strip, extends this principle by using fiber optic bend sensors spaced at regular intervals.

Functional ink-based deformation sensors [15, 19, 25, 29, 30, 24] are interesting for rapid prototyping since they can be easily fabricated through printing. Most commercial flex sensors based on conductive ink are printed as a linear pattern of carbon-based ink on a polyimide substrate with terminal connections of more conductive material, usually silver [1, 7]. The sensors function as analog resistors whose

resistance depends on the magnitude of surface flexion. These sensors exhibit a large change in resistance in the permissible bending range due to the carbon-based ink material. Also, each sensor can only sense bending along a single axis. For sensing multi-axial deformations, multiple sensors need to be laid out on the substrate which would not be possible for highly curved or narrow shapes.

Prior work has investigated deformation sensing of paper substrates using an array of commercial strain gauges [11]. Commercial strain sensors are easy to interface, but not to customize and they are not very conformal to different surface shapes.

FlexSense [29] captures bending deformations of an A4-sized flexible sheet using screen-printed piezoelectric sensors. The surface deformation is reconstructed in high fidelity through machine learning techniques. However, the sensor has a fixed geometry and involves a multi-step, multi-material screen printing process. DefSense [8] investigates computational design of 3D deformable input devices of highly custom shapes. However, the approach builds on use of resistive wires and manual assembly. In contrast, our approach addresses sensors on thin surfaces that are printed in one pass.

As one of the instant fabrication techniques, we leverage conductive inkjet printing [19], a technique for printing conductive traces directly on a paper substrate that requires no post-processing steps. Using such single layer printed patterns, various sensing modalities have been investigated, including touch sensing, pressure and proximity sensing [15]. In conjunction with other electronic components, interesting functional prototypes have been reported in [18]. Novel interaction capabilities such as robustness against cutting [26] and deformability [15] arise, since sensors are directly printed on thin and flexible substrates. In this work, we investigate flex sensing on custom shapes using inkjet-printed patterns.

## BASIC PRINCIPLE

Electrical conductivity of certain conductive materials changes with surface flexion. When such a material is subject to tensile (outward) bending, conductive particles within the material move apart from each other, increasing the overall resistance. Similarly, when the material is under compressive (inward) bending, conductive particles move closer to each other and hence overall resistance decreases [6]. The higher the magnitude of flexing, the higher is the change in resistance.

Commercial flex sensors use proprietary carbon-based ink [1, 7]. Recent work on embedded 3D printed strain gauges for flex sensing [25] used carbon conductive grease material. Graphite bounded with clay, as in pencil cores, also exhibits resistance change to flexion as demonstrated in [22]. Silver nanoparticle ink used for conductive inkjet printing also exhibits a change in resistance to flexing [19]; however it

shows a smaller response range than the more resistive carbon-based ink.

The most basic design of a flex sensor is just a single line of conductor, whose resistance is measured from its two ends. The line can also be laid out in a U shape, resulting in two parallel lines responding to flexing with a higher response than a single line. Eventually, an even longer line can be laid out in a zig-zag pattern of parallel lines to maximize the sensing lines subjected to bending in the parallel direction. Figure 2(a) illustrates the standard design. The sensor design senses bending predominantly along the direction of the parallel sensor lines, referred as the longitudinal axis. We will demonstrate how to build upon this basic principle to realize customized sensor surfaces.

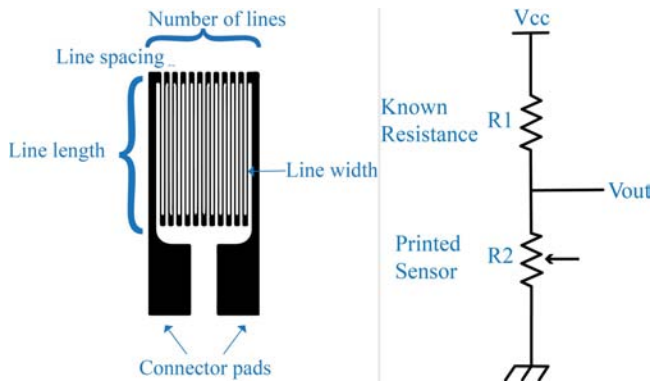


Figure 2. (a) Standard resistive flex sensor design, (b) Schematics of a voltage divider circuit

### DESIGNING AND FABRICATING A SENSING SHEET

The first step towards making a sensor sheet consisting of a single sensor or an array is preparing a digital design in any 2D vector graphics application, such as Adobe Illustrator.

The design is then fabricated using printing. We focus on conductive inkjet printing [19], however the design can also be screen-printed using appropriate ink material [28, 24]. We used Mitsubishi NBSIJ-MU01 [5] silver nanoparticle ink. We successfully used a Canon iP100 photo inkjet printer and an Epson L220 inkjet printer for printing the designs. White and transparent PET films [5] were used as substrates for printing conductive traces. Other substrates such as resin coated paper and glossy photo paper can also be used, as reported in [19]. [19] reports the thickness of silver layer on paper is around 300 nm, and the cost of printing a one meter conductive trace of 1mm width is approximately 5 US cents.

The designs are printed in a single print step, as the design consists of a single material, both for active sensing as well as end connectors. The ends of the sensor design are generally made slightly wider to attach connecting wires. We connected the printed sensors to measurement circuit using thin flat cables adhered to the design with copper tape.

The change in resistance of the sensor can be measured directly with a resistance meter or can be read by a microcontroller using a voltage divider circuit, as shown in

Figure 2(b). For single sensors and small sensor arrays, we used an Arduino Uno and for arrays requiring more I/O pins an Arduino Mega. In Figure 2(b), the resistance of the printed sensor ( $R_2$ ) is calculated by:

$$R_2 = \left( \frac{V_{cc}}{V_{out}} - 1 \right) * R_1$$

where  $R_1$  is a known resistance,  $V_{cc}$  is the supply voltage and  $V_{out}$  is the measured voltage output. The known resistance value is generally chosen to be close to the flat state resistance of the printed design. For instance, for a printed design with flat state resistance of  $500\Omega$ , a known resistance  $R_1$  of  $470\Omega$  was used.

In scenarios involving either very low resistance change of the sensor pattern or when requiring high accuracy of sensing, resistance can be measured by high resolution measurement devices as in [3, 22] or circuits such as a wheatstone bridge with amplifier as in [11, 24]. To increase robustness of the printed sensor, laminate of clear tape can be applied. This avoids moisture contact and silver being rubbed off. Other thinner laminate coating alternatives are reported in [19]. For short term usage, no laminate is required.

### DESIGN PRIMITIVES

The possibility to design a flex sensor in a vector graphics application opens up a wide space for customizing the shape. It enables novel opportunities for tangible interfaces. In this section, we give an overview of the design primitives and how these affect sensing. The design of a flex sensing geometry has the following primitives: i) number of sensing lines, ii) line length, iii) line width, iv) line spacing, v) composition and vi) connecting traces. The resistance of the pattern depends on the sensor dimensions by

$$R = \rho \frac{L}{A} \quad (1)$$

where  $L$  is the sensor length,  $A$  is the cross-sectional area and  $\rho$  is resistivity of the sensing material. The cross-sectional area is determined by line width and line thickness. Line thickness can be customized by printing a pattern multiple times.

**Number of sensing lines** The overall change in resistance of the pattern to flexing depends on the number of sensing lines. With more sensing lines, the resistance change to flexing is higher as compared to fewer sensing lines. Our sensor designs typically have 10 to 30 sensing lines. In designs where the entire shape is encased by a continuous sensor, such as crescent and leaf designs (Figure 1) the total sensing lines are more however intermediate tapping lines can be inserted to measure a more granular response.

**Line length** Sensor resistance measurement indicates the average strain across the active sensing area, hence the active line length can be matched with the target deformation curvature. Typically, the line length of our sensors varies between 2cm and 5cm.

**Line width** Line width can be customized depending on the sensing material. For more conductive materials such as silver nanoparticle ink, wider sensing lines result in a lower sensor response and are generally not preferred as more material is consumed with no advantage in sensing response. Instead, for applications that require less response range, fewer thin sensor lines can be drawn instead of a larger number of wide lines. However, commercial flex sensors are printed typically as a single wide line, as they use carbon-based ink. The typical width of our sensor designs varies between 300 $\mu$ m and 500 $\mu$ m.

**Line spacing** This primitive caters to the linear and angular spacing between the sensor lines. Each of the sensor lines need not be parallel to each other and can be placed at different angular orientations. This enables sensing multi-axial deformations. Intermediate tapping can be done for multi-axial sensing designs depending on the required sensing granularity. Figure 3 illustrates an omni-directional circular sensor.

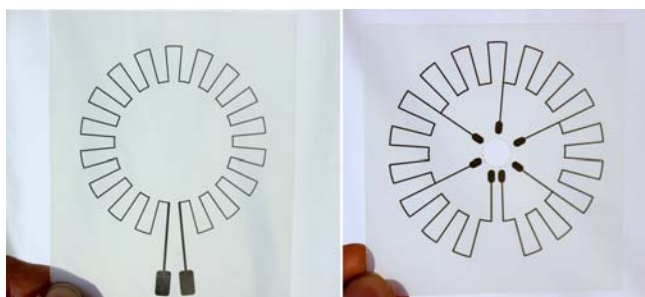


**Figure 3. An omni-directional flex sensor design (right) with intermediate tapping**

The linear spacing between the sensor lines is also customizable. Generally, the linear spacing between the sensor lines is kept much smaller than the sensor length. If the spacing is larger, then the change in resistance to flexing across sensor length is attenuated within the material laid out in perpendicular direction. In our standard design, the line spacing is slightly less than twice the line width. In other designs, the maximum spacing is 1mm except in designs such as the fish fin, where we used a considerably wider spacing to mimic the visual appearance of a caudal fin.

**Composition** This primitive captures how multiple sensing units within a geometry are laid spatially. Multiple sensing units can be laid on 1D & 2D surfaces in different geometries as described in the next section. Linear and angular spacing between each of the sensing units can be customized for different application scenarios. For instance, two sensing units in a bird shape design are slightly curved to fit the wing shape better. As another example, five sensing units arranged in a flower shape allow for multiple points of interaction on a single flower-shaped sensor. (Figure 1)

**Connecting traces** These traces connect the sensor design to the area on the substrate where contacts are tethered to a microcontroller. The connecting traces are generally quite

wide to have less resistance, and typically curved to avoid resistance change due to any uni-axial flexion.

In the next section, we discuss sensor geometries for 1D & 2D, along with interesting custom shape geometries.

### SPATIAL 1D & 2D SENSOR GEOMETRIES

A single sensor can only sense uni-radial flexing, hence to sense more complex flex deformations, multiple sensors can be arranged in different spatial arrangements. For a one-dimensional sensing strip, multiple sensing units can be arranged linearly with some spacing. For two-dimensional surfaces we propose a circular arrangement, with individual sensor units oriented in different directions. The total response of surface deformation is simply the integration of individual sensing unit responses.

Apart from these generic arrangements, the sensor geometries can be customized to suit a wide variety of custom 2D shapes. We illustrate six example patterns (Figure 1, Figure 9): inchworm, bird wing, flower, leaf, crescent and fish fin.

*Inchworm:* An inchworm design illustrates the simplest sensor design. The design spans the central body shape of a paper inchworm and can sense its curvature while it is being moved. The sensor consists of a U-shaped line design. (design dimensions: length = 62mm, line width = 0.5mm)

*Bird wing:* This design illustrates a composition of multiple sensing units. A flex sensor spanning each of the wings can capture flexion during wing flapping. Sensing lines in each unit span the wings partly and are slightly curved to better fit to the wing shape. (design dimensions: length = 45mm, width = 0.35mm, curved at 8°)

*Flower:* This design illustrates a circular arrangement of individual sensing units. The example design consists of five petals connected through a central unit. Each of the sensing units consists of varying line lengths to conform to the petal shape and is connected to the central connector. (design dimensions: length1 = 29.78mm, length2 = 35.36mm, length3 = 36.46mm, width = 0.33mm)

*Leaf design:* This design illustrates alignment of the sensing lines at an angle to better fit the target shape. A single sensor runs through the entire leaf shape. Intermediate tapping points can be added for granular sensing response. (design dimensions: leaf length: 80mm, width: 35mm, sensing lines aligned at 45°)

*Crescent design:* This design illustrates embedding a flex sensing within an extremely curved surface. Length of the sensing lines is continuously varied to adapt to the crescent shape. (design dimensions: length of crescent: 77 mm, width of crescent: 22mm, line width: 0.35mm)

*Fish design:* This design illustrates how a sensor can mimic the visual appearance of the interactive object. We illustrate a sensor placed around the caudal fin (tail) of the fish. The sensor can sense the back and forth wavy movement of the



tail. It has fewer sensing lines with varying spacing between them. (design dimensions: length of fin = 30mm, width of fin = 44mm, line width = 0.5mm)

### SPECIAL CASE OF FOLD SENSING

A fold is an extreme case of bending, resulting in an axial crease on the surface. Such a deformation causes a much higher increase in the sensor resistance. When the fold is released, the resistance value stays still considerably higher than the flat state resistance due to the permanent physical deformation of the substrate and the sensor. A fold can be sensed once through such a sharp increase in the sensor resistance. Due to the large change in resistance at a fold, the sensor pattern can be minimized to a single line design (Figure 4).

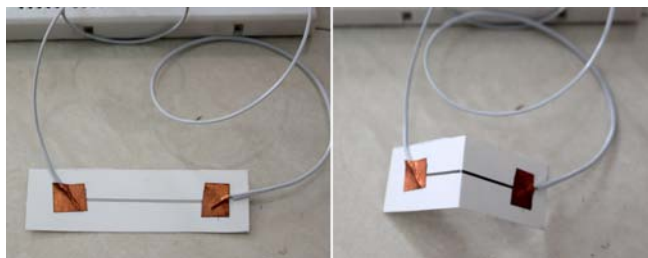


**Figure 4.** Sensing folding through single line sensors. (left) flat line, sensor released after a sharp fold at the center

An inkjet-printed trace (length = 4cm and width = 0.5mm) on a sheet of paper had a flat state resistance of 63Ω. In a completely folded state, the resistance was 356Ω (565% increase). After the sensor was released from the pinched state, the resistance still stayed at 231Ω (366% of flat state). These inexpensive and simple line sensors can be arranged at to-be-folded axes on a deformable surface for sensing the sequence of folds for a single use, as we illustrate in the applications section.

### CHARACTERIZATION AND EVALUATION

In this section, we investigate sensor response in different deformation scenarios through a set of technical experiments. We then relate the findings to answer practical questions from an interface designer's perspective: what is the sensor response at different bending curvatures, how does it compare to a commercial flex sensor, how does the sensor behave for repetitive deformations, and how does the response vary with sensor dimensions?

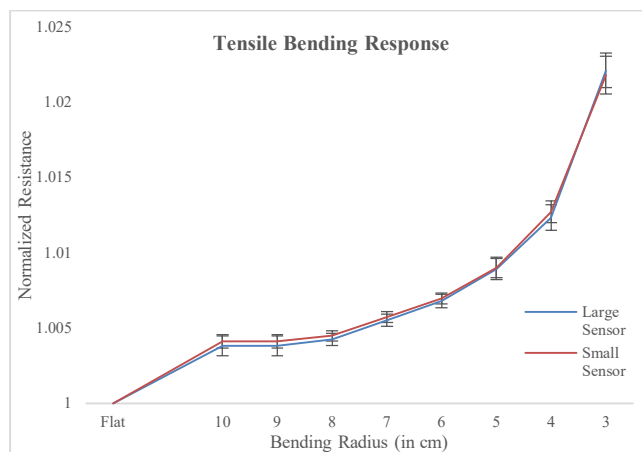
Depending on the applied deformation, sensor response falls in two categories: static and dynamic. In static deformation, the sensor moves from one state to another slowly, and it has time to settle at a state before being deformed to another state. In dynamic deformation, the sensor is deformed at a higher speed and it does not have time to settle at a particular state.

We conducted two experiments to understand the sensor response for static and dynamic deformations. We printed sensors of two sizes relevant for practical usage scenarios, as illustrated as inset in Figure 6. (*large sensor*: total length (l)

61.4 mm, sensor line length (sl) 39 mm, no. of lines (n) 22, line width (w) 0.35 mm, spacing(s) 0.65 mm, *small sensor*: 55% scaled version of the larger sensor). Three sensors of each of the sizes were printed.

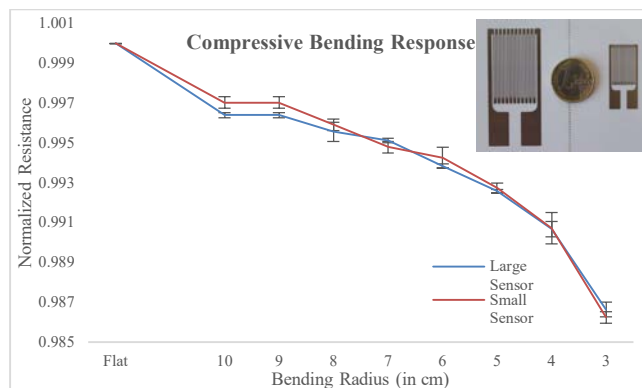
In the first experiment, we 3D-printed 7 cylinders of different curvatures (with diameter between 3-10 cm). We bent the sensors across each of them, with printed side up (tensile bending) and printed side down (compressive bending). Each sensor was flexed across a cylinder, resistance was measured and then the sensor was brought back to flat state and the process was repeated for consecutive cylinders.

Figure 5 shows the normalized ( $R/R_{\text{flat}}$ ) response of both the sensor sizes for tensile (outward) flexing. As expected, the sensor resistance increases from the flat state value with increasing curvatures (smaller bend radii). A third-degree polynomial curve fitted best to each of the responses (large sensor:  $R^2 = 0.9883$ , small sensor:  $R^2 = 0.9921$ ).



**Figure 5.** Sensor response to tensile bending

Figure 6 shows the response of sensors to compressive bending. The sensor resistance decreases from flat state for increasing curvatures, as expected. Each response can be well represented by a polynomial of third degree as it does for tensile bending (large sensor:  $R^2 = 0.9957$ , small sensor:  $R^2 = 0.9927$ ).



**Figure 6.** Sensor response to compressive bending

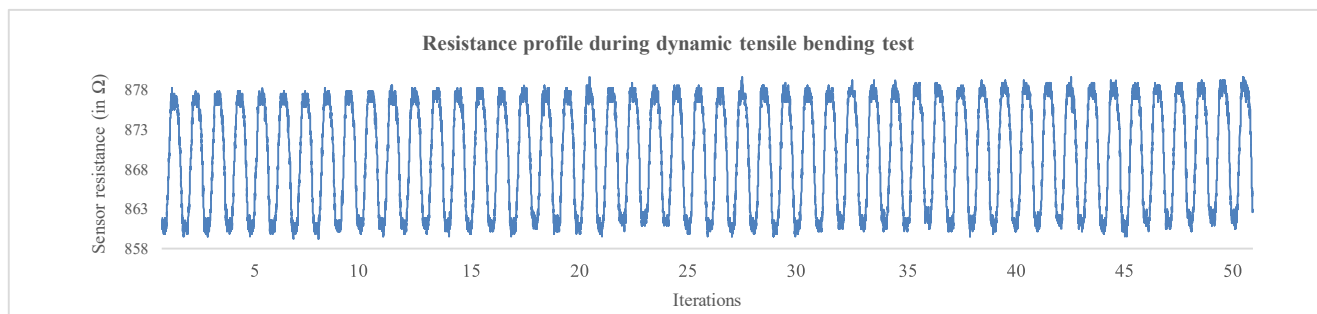


Figure 7. Sensor response during 50 iteration dynamic tensile bending test

These findings show that the sensors have a continuous response for flexing in both directions. A third-degree polynomial yields a robust mapping function of resistance to curvature in the measured range. Hence, for a sensor to be used for static deformations, the mapping can be stored beforehand, and then the measured resistance values can be used for a lookup of surface curvature.

We also find that normalized sensor response ( $R/R_{\text{flat}}$ ) for tensile and compressive bending for both the sensor sizes is quite similar. Tensile bending response is slightly higher ( $\Delta R/R_{\text{flat}} = 2.213\%$  (large sensor),  $\Delta R/R_{\text{flat}} = 2.18\%$  (small sensor)) than compressive bending response ( $\Delta R/R_{\text{flat}} = 1.34\%$  (large sensor),  $\Delta R/R_{\text{flat}} = 1.38\%$  (small sensor)).

To compare the response of our design to a commercial flex sensor, we took a 2.2 inch carbon ink-based sensor [7] and flexed it across different diameter cylinders, with printed side up and down. The sensor datasheet reports a tolerance of 30% for the resistance values. Flat state resistance of the sensor was around 21.6k $\Omega$  and the resistance at 2cm tensile radius of curvature was 58.8k $\Omega$  ( $\Delta R/R = 172.0\%$ ). The bending response of this sensor also followed a third order polynomial ( $R^2 = 0.996$ ) during tensile bending. The compressive bending response of the sensor was slightly irregular and there was no monotonous reduction in the resistance from flat state resistance. The resistance at 2cm compressive bending curvature was 19.52 k $\Omega$  ( $\Delta R/R = 11.5\%$ ). This is in-line with findings from other experiments on commercial flex sensors, which have also indicated a non-linear relation between sensor resistance and bending radius [34]. Our findings indicate that in tensile bending the range of the commercial sensor is considerably higher, related to use of carbon-based sensing material compared to silver ink. However, its response range is considerably lower and slightly irregular in compressive bending.

The next experiment was conducted to understand the sensor response for repetitive dynamic deformations. We measured the sensor response for deformations generated by a simplistic rack and pinion based dc motor setup. We took a substrate containing a large sized sensor. Both the ends of the substrate were mounted to revolute joints, to allow movement during flexion. One of the ends was kept steady while the other moved linearly through the motor, generating repetitive flexion of the substrate. The sensor was flexed fifty

times from flat state to a curvature of 2.96 cm at a speed of  $\sim 0.25\text{Hz}$ . Figure 7 shows the running average of the sensor response during the test. The average range during the iterations was found to be 16.39 $\Omega$  (standard deviation: 0.43). Since the deviation in the range and flat state resistance is small, no re-calibration of the sensor is required for applications where the acceptable error is above the observed deviation. The slight deviation in this case could be attributed to multiple factors including mechanical properties of the print paper sheet, minor irregularities in the dc motor motion and properties of the silver nanoparticle ink. Factors such as speed and extent of deformation and number of iterations also affect the sensor behavior in dynamic deformations. A detailed characterization of dynamic behavior of the sensor is beyond the scope for the present work.

Sensor dimensions affect the sensor response following equation (1), within the resolution limits of the printer. Normalized sensor response for uniformly scaled sizes described earlier has been observed to be identical. Our experience indicates that when the sensor lines are very thin ( $\leq 250\mu\text{m}$ ), the line width of closely spaced parallel lines is not very uniform when printed, i.e. few lines are slightly wider than others in prints. Sensors printed with such dimensions still work, however the resistance relation to dimensions as given by equation (1) now depends on the actual printed width of each of the lines. We achieved best sensing results with the standard design.

#### EXAMPLE APPLICATIONS

In this section, we showcase application scenarios using a single sensor as well as multi sensor 1D and 2D arrays. In the design of these application cases, we have favored simplicity over complex functionality, to showcase how creative makers who might have only little programming skills can leverage the easy-to-use printing framework for creating their custom flex sensors.

#### Curvature measurement of objects

A single sensor is well-suited to measure curvature of objects and surfaces within its responsive range. We took five objects with diameters ranging from 1.5cm to 8cm. The sensor was calibrated to an accuracy of 1cm and could correctly classify the curvature of the test objects (Figure 8).



Figure 8. Curvature measurement using a single sensor

#### Animating virtual entities through direct physical input

In this application example, we describe usage of i) a single sensor and ii) a linear 1D array. A flex sensor can be used as a direct physical input for animating virtual entities. Locomotion patterns of certain species involve flexion and we can emulate them through the sensors. We have created *Inchi*, a virtual inchworm that can be animated through direct physical input.

Radius of the motion loop can be regulated through the extent of flexion of the sensor. Since we have a bi-directional sensor, we can also associate inward and outward bending to movement of *Inchi* in forward and reverse directions (Figure 9).



Figure 9. Inchi, a virtual inchworm animated with a single flex sensor

A printed sensor containing an array of two sensing units is used to animate an emoticon. Physical shape of the sensor sheets is mapped to one of the various moods: *neutral*, *happy*, *sad*, *confused* (Figure 10).

#### Interactive paper craft

Kids can design interactive paper crafts that contain flex sensors in custom shapes. Specific deformation gestures can be mapped to audio output. For instance, flexing a bird wing can generate a flapping sound, moving the tail of a fish can generate a wave sound, humming bees can be heard when flexing the petals of a paper flower.

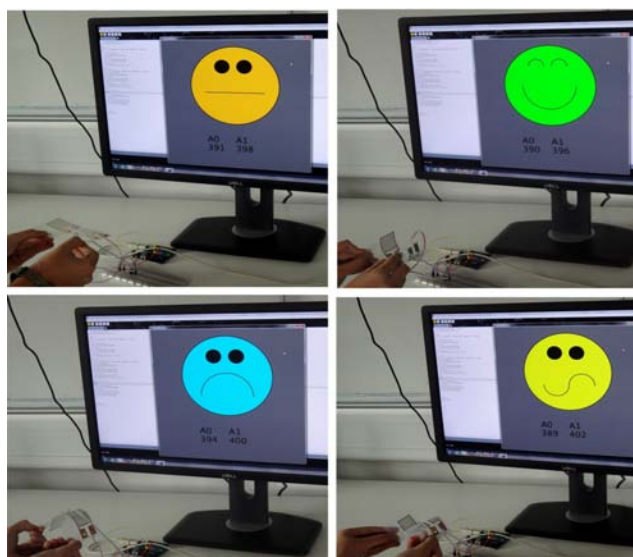


Figure 10. A two sensor linear array animating four moods of an emoticon (clockwise from top): i) neutral ii) happy iii) confused iv) sad.

#### Multimodal I/O sheet

We can integrate other sensing modalities such as touch sensing [15] and output capabilities such as LEDs along with flex sensing on a single printed sheet. Such an I/O surface allows users to build interactive objects with multimodal interaction capabilities. Figure 11 shows a sample bow shaped sheet containing two flex sensors on the side and a touch sensor in between. Each flex sensor is accompanied by a resistor to form a voltage divider. Each of the sensors have a corresponding led that glows when the sensor is interacted with (flexed or touched).

In Figure 11, left flex sensor has been bent resulting in turning the left led on. The components are adhered to the printed connectors using a conductive Z tape [19].

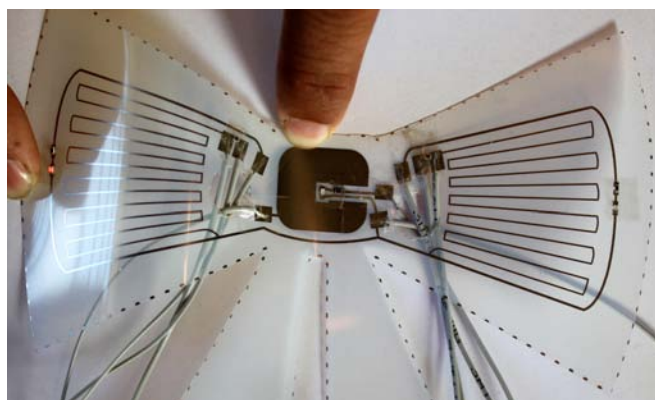


Figure 11. Printed IO Sheet with touch, flex inputs and LEDs

#### Origami training tool

In this application case, we showcase two different 2D sensor geometries. We leverage the fold sensing ability of the design. Making an origami model involves a one-time usage of specific paper surface. Inkjet-printed sensor arrays can act



as an affordable guidance tool. Novice users can be interactively guided towards the correct sequence of folds and be corrected if a step is skipped. One can alternatively use plain graphite, drawn with a pencil, to pattern it on thinner origami paper. A graphite line ( $2\text{cm} \times 0.4\text{cm}$ ) on a sheet of origami paper had a flat state resistance of  $47.7\text{k}\Omega$ . In completely folded state resistance was  $124.8\text{k}\Omega$  (261.6% increase).

We illustrate two origami shapes: boat and airplane. A boat shape can be made with box pleat folds (folds at  $90^\circ$  and  $45^\circ$ ) [10]. Figures 12(a-b) show the respective front and back sensor lines arrangements for a boat shape fold on an origami sheet. Figures 12(c-d) show the sensor lines wired with copper tape and flat cables. For the airplane design, sensors can be laid out in a radial 2D arrangement, as shown in Figure 12(e and f).

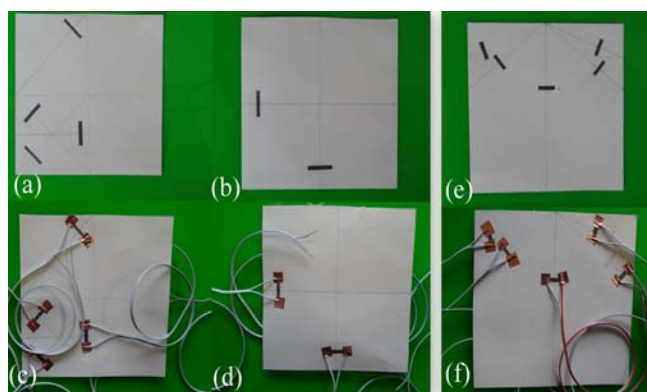


**Figure 12.** Line sensor arrangement for boat and airplane shapes: Boat (a-b) Sensor placement (front and back) with respective wiring (c-d); Airplane (e) Sensor placement with respective wiring (f).

## DISCUSSION

*Generality of the design:* The presented sensor design (also referred to as a meander line/continuous folded/sinuous pattern) has been investigated in several other electronic design architectures such as printed inductors [36] and antennas [31]. Certain styles of decorative art and architecture also inculcate such continuous line pattern [4]. Locomotion patterns in species such as fishes, snakes, worms [13] involve generation of flexion waves along the length of the body for propulsion. Wind current over sand dunes and water current on soil create meander patterns over time. Our investigation related to flex sensing in highly deformable substrates is yet an additional instance of its generality.

*Limitations:* Connectors remain a challenge for printed sensors. Connection wires add weight to the sensing surface and can affect its deformation. Even with printed connector traces, we eventually need to wire them for connection to the controller and in cases such as multi-modal IO sheet with close spacing between the connector pads, connections become quite tricky. For fold sensing of complex patterns, printed connectors can also be challenging as they would be accidentally folded while making the origami shape. Silver

nanoparticle ink demonstrates a small resistance change to flexing due to its high conductivity, which in turn requires the design to have multiple thin sensing lines for a measurable, repetitive response. This leads to a slightly wider flex sensing design compared to commercial flex sensors which are relatively narrower. Scalability of sensor designs is essentially limited by the effective printing resolution (we recommend a trace width above  $250\ \mu\text{m}$  when using our printer) and by the number of analog input pins of the microcontroller.

*Directions of future work:* Design of an automated tool for generating sensor designs including printed connectors, for user-defined shapes and materials will be an interesting direction for future research. Exploration of different connection mechanisms for printed sensors, such as vias to connect different layers of a printed sheet would be interesting. Once a wider set of functional materials can be printed with inexpensive printers, it will be relevant to explore their characteristics for custom-designed flex sensors. Advances in 3D printing of functional materials will make 3D printed designs a further interesting avenue for future work.

## CONCLUSION

In this work, we presented the design and fabrication of shape-customizable flex sensing patterns. The sensor can be designed digitally and printed. It offers the unique advantages of visual customizability, single and multi-axial flex sensing, single material and single step fabrication, and low cost. Moreover, it is easy to interface with for non-experts. We also presented different spatial arrangements of the sensor in 1D and 2D and showed how they can be used for tangible user interfaces. We believe that the design and fabrication guidelines will aid HCI researchers, practitioners, designers and makers to quickly, easily and cheaply realize deformable sensors and in-turn open new avenues of interactivity.

## ACKNOWLEDGEMENTS

This work has been partially funded by the German Research Foundation under award number EXC 284: Multimodal Computing and Interaction. We would like to thank Virendra Ashiwal, Narayan Rangarajan and Mayuresh Sarpotdar for their valuable and timely technical feedback and support.



## REFERENCES

1. Flexpoint bend sensor. Retrieved January 22, 2017 from <http://www.flexpoint.com/>.
2. How to make a fabric bend sensor. Retrieved January 22, 2017 from <http://www.kobakant.at/DIY/?p=20>.
3. Keithley 2400 source meter. Retrieved January 22, 2017 from <http://www.tek.com/keithley-source-measure-units/keithley-smu-2400-series-sourcemeter>.
4. Meander pattern. Retrieved January 22, 2017 from [https://en.wikipedia.org/wiki/Meander\\_\(art\)](https://en.wikipedia.org/wiki/Meander_(art)).
5. Mitsubishi silver nano inkjet system. Retrieved January 22, 2017 from <http://diamond-jet.com/silvernanoinkjetsystem.aspx>.
6. Sensor wiki flexion. Retrieved January 22, 2017 from <http://www.sensorwiki.org/doku.php/sensors/flexion>.
7. Spectra symbol bend sensor. Retrieved January 22, 2017 from <http://www.spectrasymbol.com/flex-sensor>.
8. Moritz Bächer, Benjamin Hepp, Fabrizio Pece, Paul G. Kry, Bernd Bickel, Bernhard Thomaszewski, and Otmar Hilliges. Defsense: Computational design of customized deformable input devices. In *Proceedings of the 2016 CHI Conference on Human Factors in Computing Systems*, CHI '16, 3806–3816. <http://doi.acm.org/10.1145/2858036.2858354>
9. Ravin Balakrishnan, George Fitzmaurice, Gordon Kurtenbach, and Karan Singh. Exploring interactive curve and surface manipulation using a bend and twist sensitive input strip. In *Proceedings of the 1999 Symposium on Interactive 3D Graphics*, I3D '99, 111–118. <http://doi.acm.org/10.1145/300523.300536>
10. Nadia Benbernou, Erik D. Demaine, Martin L. Demaine, and Aviv Ovadya. A universal crease pattern for folding orthogonal shapes. *CoRR*, abs/0909.5388, 2009. <http://arxiv.org/abs/0909.5388>
11. Chin-yu Chien, Rong-Hao Liang, Long-Fei Lin, Liwei Chan, and Bing-Yu Chen. Flexibend: Enabling interactivity of multi-part, deformable fabrications using single shape-sensing strip. In *Proceedings of the 28th Annual ACM Symposium on User Interface Software & Technology*, UIST '15, 659–663. <http://doi.acm.org/10.1145/2807442.2807456>
12. Artem Dementyev, Hsin-Liu (Cindy) Kao, and Joseph A. Paradiso. Sensortape: Modular and programmable 3d-aware dense sensor network on a tape. In *Proceedings of the 28th Annual ACM Symposium on User Interface Software & Technology*, UIST '15, 649–658. <http://doi.acm.org/10.1145/2807442.2807507>
13. Kelly M. Dorgan, Chris J. Law, and Greg W. Rouse. Meandering worms: mechanics of undulatory burrowing in muds. In *Proceedings of the Royal Society of London B: Biological Sciences*, 280(1757), 2013. <http://dx.doi.org/10.1098/rspb.2012.2948>
14. David T. Gallant, Andrew G. Seniuk, and Roel Vertegaal. Towards more paper-like input: Flexible input devices for foldable interaction styles. In *Proceedings of the 21st Annual ACM Symposium on User Interface Software and Technology*, UIST '08, 283–286. <http://doi.acm.org/10.1145/1449715.1449762>
15. Nan-Wei Gong, Jürgen Steimle, Simon Olberding, Steve Hodges, Nicholas Edward Gillian, Yoshihiro Kawahara, and Joseph A. Paradiso. Printsense: A versatile sensing technique to support multimodal flexible surface interaction. In *Proceedings of the SIGCHI Conference on Human Factors in Computing Systems*, CHI '14, 1407–1410. <http://doi.acm.org/10.1145/2556288.2557173>
16. Daniel Groeger, Elena Chong Loo, and Jürgen Steimle. Hotflex: Post-print customization of 3d prints using embedded state change. In *Proceedings of the 2016 CHI Conference on Human Factors in Computing Systems*, CHI '16, pages 420–432. <http://doi.acm.org/10.1145/2858036.2858191>
17. Gero Herkenrath, Thorsten Karrer, and Jan Borchers. Twend: Twisting and bending as new interaction gesture in mobile devices. In *CHI '08 Extended Abstracts on Human Factors in Computing Systems*, CHI EA '08, pages 3819–3824, New York, NY, USA, 2008. <http://doi.acm.org/10.1145/1358628.1358936>
18. Y. Kawahara, S. Hodges, Nan-Wei Gong, S. Olberding, and J. Steimle. Building functional prototypes using conductive inkjet printing. *Pervasive Computing, IEEE*, 13(3):30–38, July 2014. <http://doi.org/10.1109/MPRV.2014.41>
19. Yoshihiro Kawahara, Steve Hodges, Benjamin S. Cook, Cheng Zhang, and Gregory D. Abowd. Instant inkjet circuits: Lab-based inkjet printing to support rapid prototyping of ubicomp devices. In *Proceedings of the 2013 ACM International Joint Conference on Pervasive and Ubiquitous Computing*, UbiComp '13, 363–372. <http://doi.acm.org/10.1145/2493432.2493486>
20. Johan Kildal, Susanna Paasovaara, and Viljakaisa Aaltonen. Kinetic device: Designing interactions with a deformable mobile interface. In *CHI '12 Extended Abstracts on Human Factors in Computing Systems*, CHI EA '12, 1871–1876. <http://doi.acm.org/10.1145/2212776.2223721>

21. Byron Lahey, Audrey Girouard, Winslow Burleson, and Roel Vertegaal. Paperphone: Understanding the use of bend gestures in mobile devices with flexible electronic paper displays. In *Proceedings of the SIGCHI Conference on Human Factors in Computing Systems*, CHI '11, 1303–1312.  
<http://doi.acm.org/10.1145/1978942.1979136>
22. Cheng-Wei Lin, Zhibo Zhao, Jaemyung Kim, and Jiaying Huang. Pencil drawn strain gauges and chemiresistors on paper. *Scientific Reports*, 4:3812, January 2014.  
<http://dx.doi.org/10.1038/srep03812>
23. J. Lo and A. Girouard. Fabricating bendy: Design and development of deformable prototypes. *IEEE Pervasive Computing*, 13(3):40–46, July 2014.  
<http://doi.org/10.1109/MPRV.2014.47>
24. Joanne Lo, Doris Jung Lin Lee, Nathan Wong, David Bui, and Eric Paulos. Skintillates: Designing and creating epidermal interactions. In *Proceedings of the 2016 ACM Conference on Designing Interactive Systems*, DIS '16, 853–864.  
<http://doi.acm.org/10.1145/2901790.2901885>
25. Joseph T. Muth, Daniel M. Vogt, Ryan L. Truby, Yiğit Mengüç, David B. Kolesky, Robert J. Wood, and Jennifer A. Lewis. Embedded 3d printing of strain sensors within highly stretchable elastomers. *Advanced Materials*, 26(36):6307–6312, 2014.  
<http://dx.doi.org/10.1002/adma.201400334>
26. Simon Olberding, Nan-Wei Gong, John Tiab, Joseph A. Paradiso, and Jürgen Steimle. A cuttable multi-touch sensor. In *Proceedings of the 26th Annual ACM Symposium on User Interface Software and Technology*, UIST '13, 245–254.  
<http://doi.acm.org/10.1145/2501988.2502048>
27. Simon Olberding, Sergio Soto Ortega, Klaus Hildebrandt, and Jürgen Steimle. Foldio: Digital fabrication of interactive and shape-changing objects with foldable printed electronics. In *Proceedings of the 28th Annual ACM Symposium on User Interface Software & Technology*, UIST '15, 223–232.  
<http://doi.acm.org/10.1145/2807442.2807494>
28. Simon Olberding, Michael Wessely, and Jürgen Steimle. Printscreen: Fabricating highly customizable thin-film touch-displays. In *Proceedings of the 27th Annual ACM Symposium on User Interface Software and Technology*, UIST '14, 281–290.  
<http://doi.acm.org/10.1145/2642918.2647413>
29. Christian Rendl, David Kim, Sean Fanello, Patrick Parzer, Christoph Rhemann, Jonathan Taylor, Martin Zirkel, Gregor Scheipl, Thomas Rothländer, Michael Haller, and Shahram Izadi. Flexsense: A transparent self-sensing deformable surface. In *Proceedings of the 27th Annual ACM Symposium on User Interface Software and Technology*, UIST '14, 129–138.  
<http://doi.acm.org/10.1145/2642918.2647405>
30. Christian Rendl, David Kim, Patrick Parzer, Sean Fanello, Martin Zirkel, Gregor Scheipl, Michael Haller, and Shahram Izadi. Flexcase: Enhancing mobile interaction with a flexible sensing and display cover. In *Proceedings of the 2016 CHI Conference on Human Factors in Computing Systems*, CHI '16, 5138–5150.  
<http://doi.acm.org/10.1145/2858036.2858314>
31. Analisa Russo, Bok Yeop Ahn, Jacob J. Adams, Eric B. Duoss, Jennifer T. Bernhard, and Jennifer A. Lewis. Pen-on-paper flexible electronics. *Advanced Materials*, 23(30):3426–3430, 2011.  
<http://dx.doi.org/10.1002/adma.201101328>
32. Martin Schmitz, Mohammadreza Khalilbeigi, Matthias Balwierz, Roman Lissermann, Max Mühlhäuser, and Jürgen Steimle. 2015. Capricate: A Fabrication Pipeline to Design and 3D Print Capacitive Touch Sensors for Interactive Objects. In *Proceedings of the 28th Annual ACM Symposium on User Interface Software & Technology* (UIST '15), 253–258.  
<http://dx.doi.org/10.1145/2807442.2807503>
33. Carsten Schwesig, Ivan Poupyrev, and Eijiro Mori. Gummi: A bendable computer. In *Proceedings of the SIGCHI Conference on Human Factors in Computing Systems*, CHI '04, 263–270.  
<http://doi.acm.org/10.1145/985692.985726>
34. Lisa Simone, Derek G. Kamper. Design considerations for a wearable monitor to measure finger posture. *Journal of NeuroEngineering and Rehabilitation*, 2(1):5, 2005.  
<http://dx.doi.org/10.1186/1743-0003-2-5>
35. Jürgen Steimle, Andreas Jordt, and Pattie Maes. Flexpad: Highly flexible bending interactions for projected handheld displays. In *Proceedings of the SIGCHI Conference on Human Factors in Computing Systems*, CHI '13, 237–246.  
<http://doi.acm.org/10.1145/2470654.2470688>
36. Victor Torres, Ruben Ortuno, Pablo Rodriguez-Ulibarri, Amadeu Griol, Alejandro Martinez, Miguel Navarro-Cia, Miguel Beruete, and Mario Sorolla. Mid-infrared plasmonic inductors: Enhancing inductance with meandering lines. *Sci. Rep.*, 4:–, January 2014.  
<http://dx.doi.org/10.1038/srep03592>
37. Jun-ichiro Watanabe, Arito Mochizuki, and Youichi Horry. Booksheet: Bendable device for browsing content using the metaphor of leafing through the pages. In *Proceedings of the 10th International Conference on Ubiquitous Computing*, UbiComp '08, 360–369.  
<http://doi.acm.org/10.1145/1409635.1409684>